Contrib Mineral Petrol (2003) 146: 275–285
DOI 10.1007/s00410-003-0501-y

ORIGINAL PAPER

Natalie C. Caciagli · Craig E. Manning

The solubility of calcite in water at 6–16 kbar and 500–800 °C

Received: 14 August 2002 / Accepted: 19 June 2003 / Published online: 10 October 2003
© Springer-Verlag 2003

Abstract The solubility of calcite in H_2O was measured at 6–16 kbar, 500–800 °C, using a piston-cylinder apparatus. The solubility was determined by the weight loss of a single crystal and by direct analysis of the quench fluid. Calcite dissolves congruently in the pressure (P) and temperature (T) range of this study. At 10 kbar, calcite solubility increases with increasing temperature from 0.016 ± 0.005 molal at 500 °C to 0.057 ± 0.022 molal at 750 °C. The experiments reveal evidence for hydrous melting of calcite between 750 and 800 °C. Solubilities show only a slight increase with increasing P over the range investigated. Comparison with work at low P demonstrates that the P dependence of calcite solubility is large between 1 and 6 kbar, increasing at 500 °C from 1.8×10^{-5} molal at 1 kbar to 6.4×10^{-3} molal at 6 kbar. The experimental results are described by:

$$\log m_{CacO_3} = -3.95 + 0.00266T + (32.8 - 0.0280T)\log \rho_{H_2O}$$

where T is in Kelvin and ρ_{H2O} is the density of pure water in g/cm^3. The equation is applicable at 1–20 kbar and 400–800 °C, where calcite and H_2O stably coexist. Extrapolated thermodynamic data for HCO_3^- indicates that the dominant dissolved carbon species is $CO_{2,aq}$ at all experimental conditions. The results require that equilibrium constant for the reaction:

$$\underset{\text{calcite}}{CaCO_3} + 2H^+ = Ca^{+2} + CO_{2,aq} + H_2O$$

increases by several orders of magnitude between 1 and 6 kbar, and also rises with isobaric T increase. Published thermodynamic data for aqueous species fail to predict this behavior. The increase in calcite solubility with P and T demonstrates that there is a strong potential for calcite precipitation during cooling and decompression of water-rich metamorphic fluids sourced in the middle to lower crust.

Editorial responsibility: T.L. Grove

N. C. Caciagli (✉) · C. E. Manning
Department of Earth and Space Sciences,
University of California at Los Angeles,
Los Angeles, CA 90095, USA
E-mail: caciagli@geology.utoronto.ca

N. C. Caciagli
Department of Geology, University of Toronto,
Toronto, M5S 3B1 Canada

Introduction

Calcite, the primary reservoir for carbon in the continental crust, is sparingly soluble in pure H_2O at low pressures and temperatures. However, the widespread occurrence of calcite-bearing veins in metamorphic rocks and ore deposits indicates that crustal fluids have the capacity to dissolve and transport significant quantities of calcium carbonate. Quantitative understanding of the links between calcite-fluid interaction during metamorphism and carbon cycling require knowledge of the solubility of calcite in H_2O at high pressure and temperature.

Previous experimental studies of the solubility of calcite in H_2O have focused on relatively low pressures and temperatures. Early work determined calcite solubility in H_2O (CO_2-free or equilibrated with Earth's atmosphere) from 25 to 370 °C along the H_2O liquid-vapor saturation curve (Wells 1915; Frear and Johnston 1926; Schloemer 1952; Morey 1962). These studies showed that calcite dissolves congruently in pure H_2O, and that solubility decreases with increasing temperature. Walther and Long (1986) and Fein and Walther (1989) measured calcite solubility in H_2O to 600 °C and 3 kbar. They observed a decrease in solubility with increasing temperature at 1–2 kbar; however at 3 kbar calcium concentration increased slightly from $10^{-3.3}$ mol solute per kg H_2O (molal) at 550 °C to $10^{-3.1}$ molal at 600 °C.

Fein and Walther (1987, 1989) inferred that, from 100 to 600 °C and 1–3 kbar in pure water, Ca^{+2} is the predominant calcium species, with $CaOH^+$, $CaHCO_3^+$ and

$CaCO_{3,aq}$ representing an insignificant fraction of the total dissolved Ca. Thus, calcite solubility in pure H_2O at these conditions is governed by the equilibria:

$$\underset{\text{calcite}}{CaCO_3} + 2H^+ = Ca^{+2} + CO_{2,aq} + H_2O \quad (1)$$

$$CO_{2,aq} + H_2O = HCO_3^- + H^+ \quad (2)$$

$$HCO_3^- = H^+ + CO_3^{-2} \quad (3)$$

$$H_2O = H^+ + OH^- \quad (4)$$

where $CO_{2,aq}$ represents the neutral species regardless of the hydration state. Fein and Walther (1987, 1989) found that the only significant C species were $CO_{2,aq}$ and HCO_3^-. The results of Fein and Walther (1987, 1989), combined with those of Walther and Long (1986), show that at upper crustal metamorphic conditions, dissolved Ca (as Ca^{+2}) and C (as $CO_{2,aq}$ and HCO_3^-) concentrations in H_2O in equilibrium with calcite are generally low ($< 10^{-3}$ mol/kg H_2O), and that concentrations decreasing as temperature increases isobarically. Their results also suggest that isothermal increases in pressure enhance the solubility of calcite in H_2O, indicating that calcite may be substantially more soluble at mid- to lower-crustal metamorphic conditions. Although experimental studies of calcite solubility have been extended to complex aqueous solutions involving, for example, CO_2 and NaCl, at low pressures (e.g., Miller 1952; Ellis 1959; Segnit et al. 1962; Ellis 1963; Sharp and Kennedy 1965; Malinin and Kanukov 1972; Plummer and Busenberg 1982; Fein and Walther 1987, 1989), we are unaware of any previous measurement of the solubility of calcite in pure H_2O at > 3 kbar.

The present work was undertaken to measure the solubility of calcite in pure H_2O at 500 to 800 °C and 6 to 16 kbar. This study greatly extends the temperature and pressure range of calcite solubility measurements in H_2O, permitting assessment of the thermodynamic data on carbonic fluids in the Earth's crust and upper mantle. The results of the present work complement the study of calcite solubility in H_2O–NaCl fluids by Newton and Manning (2002).

Methods

If calcite dissolves congruently—i.e., all components are lost to solution in stoichiometric proportion—solubility can be measured in two ways: from the weight loss of calcite crystals equilibrated with initially pure H_2O, and from the concentration of Ca in experimental solutions. The experiments were designed to permit assessment of congruent dissolution and determination of solubility using both methods.

Experimental procedure

Natural calcite crystals from Rodeo, Durango, Mexico, were used in all experiments (Table 1). Handpicked, inclusion-free crystals were rounded in an air driven sphere grinder to minimize crushing during experiments (Bond 1951). The rounded crystals were washed for 15 s in 2.5 N HCl to dissolve adhering fines. Examples of starting materials are shown in Fig. 1A, B. For each experiment a single rounded crystal was weighed and placed in a 2-mm outer diameter (OD) perforated Pt capsule, which was then crimped tightly shut. The capsule, which served to contain all crystal fragments in the event of breakage, was weighed and then loaded in a 5-mm OD Pt outer capsule with $\backsim 50$ μL of ultrapure H_2O. Although no special measures were taken to remove atmosphere-derived CO_2 from the H_2O, its affects are insignificant ($< 10^{-5}$ molal, assuming equilibrium) at the high solubilities measured in this study ($\sim 10^{-2}$ molal). The outer Pt capsule was crimped, weighed to determine the amount of H_2O delivered, sealed by arc welding, and reweighed to check the H_2O content. Finally, the crimped portion of the outer capsule was folded to make a packet approximately 5×5×3 mm. All weighing was done on a Mettler M3 microbalance with $1\sigma = 0.003$ mg for each weighing step (determined by repeated weighing of a known mass).

Table 1 Electron microprobe analysis of starting material

	wt%
CaO	55.73(39)
FeO	0.07(11)
MgO	bd
MnO	bd
CO_2	44.20(39)
Total	100.00

Numbers in parenthesis are the standard deviations of ten analyses; *bd* below detection limit (0.05 wt%); CO_2 by difference; total normalized to 100%

The experiments were conducted in a 2.54-cm-diameter end-loaded piston-cylinder apparatus (Boyd and England 1960) using a cylindrical graphite heater and NaCl pressure cells similar to those described by Bohlen (1984). Pressure was achieved using the piston-out technique, in which assemblies were first cold pressurized to 60–70% of the final value before the temperature was increased. The thermal expansion of the assemblies during subsequent heating raised the pressure to the desired level. Under these conditions, NaCl pressure cells are frictionless and therefore no pressure correction is necessary (Johannes 1973; Bohlen 1984; Manning and Boettcher 1994). The long dimension of the Pt capsule was placed normal to the long axis of the heater to minimize the effects of temperature gradients (Newton and Manning 2000). Manning and Boettcher (1994) determined T gradients of ≤ 8 °C using the same furnace design but capsules more than twice as long in the vertical dimension; T gradients were therefore likely no more than several degrees centigrade. Temperatures were monitored with Pt-$Pt_{90}Rh_{10}$ thermocouples, which were in close contact with the Pt capsule (commonly leaving a dimpled impression on the top surface). Temperatures were not corrected for the effect of pressure on EMF.

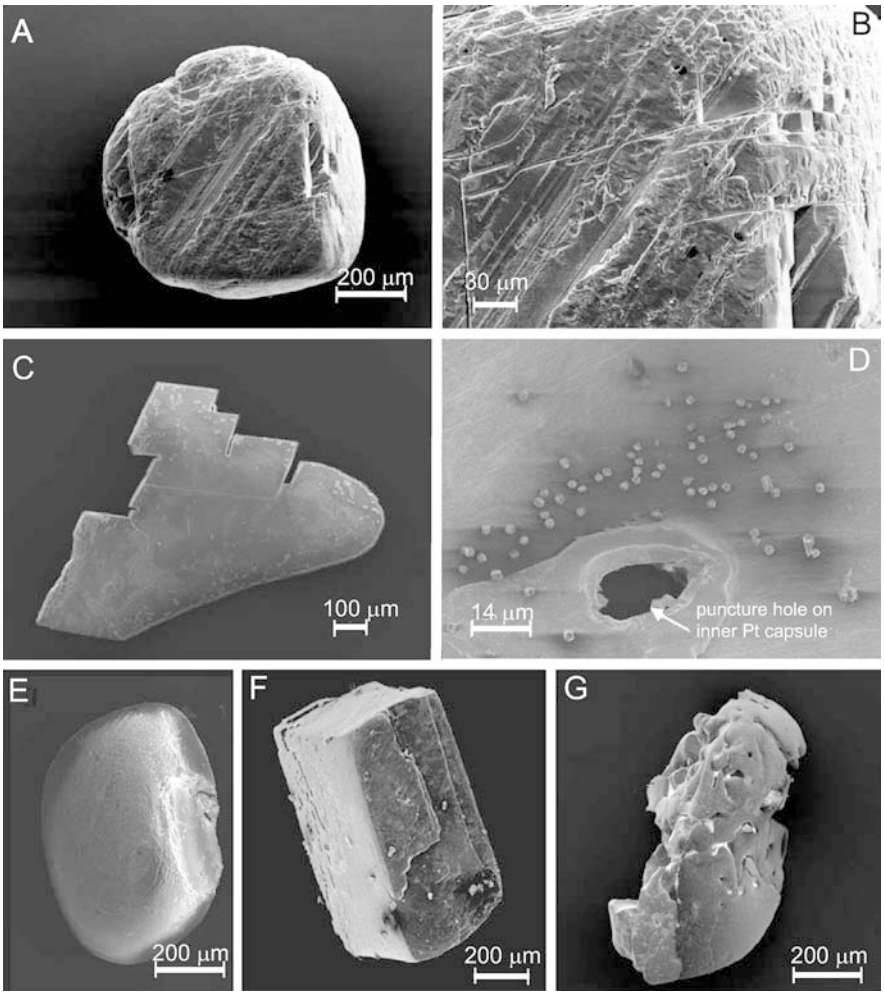

Fig. 1 Scanning electron micrographs of starting and run-product calcite crystals. **A**, **B** Example of an air-abraded and acid-etched starting calcite crystal. **C** Type-1 crystal from experiment CW-33. Crystal is thin, platy and curved, mimicking the surface of the outer Pt capsule on which it grew. **D** Type-2 crystals on the inside surface of the inner Pt capsule. The crystals are clustered around the perforations and crimped edges of the capsule. **E** Example of run-product calcite crystal displaying smooth, solution-rounded surfaces. **F** Example of run-product calcite crystal displaying evidence of dissolution and recrystallization. **G** Example of run-product calcite crystal from high-solubility experiment displaying pitted and anhedral texture

Experiments were quenched by cutting power to the heater, which resulted in temperatures dropping to 100 °C in under 30 s. The capsule was then washed in 6 N HCl in an ultrasonic cleaner for 15 min to remove any debris from the outer surface, and dried in a 115 °C oven and weighed to check for any water loss during the experiment.

To extract the experimental solution, the cleaned capsule was submerged in 2 mL of ultrapure H_2O, punctured two to three times and allowed to equilibrate for 24 h (Manning and Boettcher 1994). After removing the capsule from the extraction vessel, the solution was acidified with 8 mL of 6.6% HNO_3 and then analyzed for Ca by inductively coupled plasma atomic emission spectroscopy (ICP-AES). Owing to the small volume of the extracted samples, only three to five replicates were analyzed for each sample. Analytical errors from ICP measurements (1σ) were typically on the order of 1% relative.

After fluid extraction, the capsule was again dried in an 115 °C oven, weighed and the H_2O content of the capsule rechecked by difference. This calculation, allowing for loss of stoichiometric CO_2, typically agreed with the pre-run weight determination to within 0.7%. The capsule was then opened and the inner capsule and solid products were retrieved, weighed, and mounted for optical and SEM petrography.

Analysis and determination of solubility

Initially the experiments were conducted following the procedure of Anderson and Burnham (1965), where calcite solubility was calculated from the measured weight loss of a perforated inner capsule. This method assumes that all weight loss of the inner capsule is due to dissolution of the contained calcite crystal and that the fluid retains all dissolved calcite. The weight change of the capsule was used instead of that of the crystal because in some cases crystals broke during experiments, and it proved difficult to ensure that all calcite chips were collected for weighing.

As a check on the results obtained by weight-loss measurements, solubilities were also determined for ~2/3 of the experiments from the amount of dissolved Ca in the extracted fluids. Early experiments indicated that solubilities calculated from fluid compositions were 1 to 1.5 orders of magnitude lower than when calculated

from weight-loss. The weight-loss data also displayed considerable scatter. Investigation of the quenched capsules by scanning electron microscope (SEM) revealed two morphologically distinct types of newly formed calcite crystals on the walls of the inner and outer capsules. Type-1 crystals were relatively large (~1 mm in length). In experiments done at temperatures greater than 700 °C, these crystals are typically thin and platy, and conformed to the surface of the capsule on which they had crystallized (Fig. 1C). At temperatures less than 700 °C, the crystals tended to be euhedral rhombs. The total mass of these crystals in a single experiment ranged from 3 μg to 1 mg, with the greater masses typically occurring at higher temperatures. Transmitted light microscopy revealed that type-1 crystals were single birefringent grains. Because of their small number, relatively large size, and interface controlled growth, these crystals were interpreted as the product of transport and re-precipitation of material due to minor concentration differences imparted by the small temperature gradient in the capsule. The conclusion that type-1 crystals grew during experiments at high P–T requires that their weight be included with the original crystals in the determination of solubility by weight loss.

Crystals of the second textural group (type 2) were much smaller, less than 10 μm in length (Fig. 1D). They were distributed throughout both inner and outer Pt capsules, and covering the original calcite crystal and the type-1 crystals. Type-2 crystals varied in morphology from discrete euhedral rhombs to radiating, acicular clusters. The occurrence of a large number of small crystals suggests a transport-limited process, as would be expected with a large degree of under-cooling during growth. Hence, type-2 crystals are interpreted as quench material because of their uniform size, high nucleation density, and their even distribution on all surfaces including the original crystal and the type-1 crystals.

The presence of type-1 and type-2 calcite crystals offers an explanation for the discrepancy between solubilities calculated from fluid chemistry and solubilities calculated by weight loss. In accordance with the interpretation that type-1 crystals grew at high T and P, and type-2 crystals grew during quench, solubilities were calculated from:

$$m_{\mathrm{CacO_3}} = \frac{1000\left[w_{ic}^{i} - (w_{ic}^{f} + w_1)\right]}{100.078\ w_{\mathrm{H_2O}}} \qquad (5)$$

where $m_{\mathrm{CacO_3}}$ is the concentration of calcite in solution in units of molality, w_{ic}^{i} and w_{ic}^{f} are respectively the initial and final masses of the perforated inner capsule, w_1 is the mass of type-1 crystals, $w_{\mathrm{H_2O}}$ is the mass of water present in the experiment, and 100.078 is the molecular weight of calcite (all masses in milligrams). Equation (3) ignores type-2 crystals included in the inner capsule. Because the volume of water in the inner capsule is only several percent of the total volume of fluid in the experiment, the weights of inner-capsule type-2 crystals should be negligible (see below).

Similarly, type-2 crystals must be recombined with the solution for accurate solubility determination by fluid analysis. The quench fraction was extracted by washing the inner and outer Pt capsules in 8 mL of 6.6% HNO_3 for 20 min in an ultrasonic cleaner after extraction of the original and type-1 calcite crystals. This treatment dissolved the smaller, quench crystals adhering to the capsule walls. The quench crystals adhering to the type-1 crystals and the original crystal were too small, less than 10 μm in length, to be recovered independent of the larger crystals, and so the mass of the type-1 and original calcite crystal are increased somewhat. Assuming an even distribution of type-2 crystals on all surfaces this amounts to less than 5% of the total mass of quench material being included with the mass of type-1 crystals. The wash solution was collected and analyzed for Ca by ICP-AES and the result was added to the Ca concentration determined for the quench fluid.

Results

Experimental results are given in Table 2. Run products consisted of extracted fluid, type-1 crystals (Fig. 1C), type-2 crystals (Fig. 1D), and the original calcite crystal (Fig. 1E–G). Run-product crystals in experiments done at the conditions where solubility was highest (750 °C) were anhedral, with wormy pits and groves (Fig. 1G). Except at 800 °C, 10 kbar, where melt was interpreted to be present (see below), no other solid phases were observed, showing that calcite dissolves congruently. The absence of graphite in the quenched charges indicates that oxygen fugacity was in excess of the CCO buffer, and therefore reduced carbon species, such as CH_4 or CO, are insignificant, based on COH fluid speciation calculations (Holland and Powell 1991).

Table 2 gives the weights used in determining solubility from Eq. (5), as well as the concentrations in the quench fluid and the wash used to redissolve type-2 crystals. The weights of type-1 crystals increase with increasing solubility and range from 0 to ~90% of the weight change of the inner capsule, with an average of 44%. This indicates that type-1 crystals represent a significant fraction of the total weight change registered in the experiments. The Ca concentration in the wash solutions also increases with increasing solubility, but it is in each case higher than that in the extracted quench fluid, indicating that most of the dissolved Ca and C precipitate upon quench.

Comparison of the two independent measures of solubility offers a mass-balance test for experimental accuracy. Table 2 shows that if type-1 crystals are not included in the weight-loss calculations the solubility calculated from weight loss is greater than the solubility as calculated from fluid composition. Similarly, if quench material is not included in the calculations of fluid composition, the solubility is less than that calculated from weight loss. However, if type-1 crystals are

Table 2 Experimental results

Exp. no.	T (°C)	P (kbar)	Time (hr)	Initial calcite (mg)	Initial inner capsule (mg)	Initial H_2O (mg)	Final inner capsule (mg)	Type 1 crystals (mg)	Solubility by wt. loss (10^3*m_{CaCO3})	Extracted fluid (10^3*m_{Ca})	Type 2 crystals (10^3*m_{Ca})	Solubility by fluid analysis (10^3*m_{Ca})	Notes
CW-83	500	6	29	0.901	82.010	50.097	81.964	0.014	6.4(8)	1.75(2)	7.19(5)	8.94(5)	
CW-85	500	8	16	0.806	82.204	49.944	82.115	0.000	17.8(8)	3.71(1)	12.80(9)	16.51(9)	
CW-43	500	10	47	1.924	51.372	50.332	51.298	0.000	14.7(8)	-	-	-	
CW-44	500	10	71	2.984	51.170	50.037	51.121	0.000	9.8(8)	2.27(4)	-	-	
CW-45	500	10	95	0.823	60.505	50.593	60.470	0.000	6.9(8)	1.56(4)	-	-	
CW-72	500	10	48	2.295	74.305	48.990	74.261	0.000	9.0(9)	3.42(3)	3.73(4)	7.15(5)	
CW-66	550	10	73.5	0.639	64.043	50.566	63.782	0.175	17.0(8)	4.18(1)	-	-	
CW-67	550	10	48	0.758	73.959	49.765	73.718	0.173	13.7(9)	4.45(4)	9.51(6)	13.96(7)	
CW-87	600	6	33	0.770	84.471	49.922	84.405	0.024	8.4(8)	4.76(2)	14.84(6)	19.60(6)	
CW-89	600	8	28	0.588	76.896	50.046	76.850	0.000	9.2(8)	1.98(2)	6.40(7)	8.38(7)	
CW-63	600	10	47	0.912	72.425	49.659	72.354	0.003	13.7(9)	5.24(15)	-	-	
CW-64	600	10	37	1.502	88.569	48.861	88.373	0.027	34.6(9)	9.72(17)	-	-	
CW-71	600	10	48.6	1.169	66.967	50.578	66.716	0.188	12.4(8)	4.03(6)	11.22(9)	15.25(11)	
CW-92	600	12	25	0.620	74.607	49.553	74.468	0.000	28.0(9)	1.77(5)	20.17(12)	21.94(13)	
CW-90	600	16	21	0.344	56.182	49.916	56.045	0.003	26.8(8)	-	-	-	
CW-61	650	10	48	2.069	63.628	49.488	63.010	0.457	32.5(9)	9.03(3)	-	-	
CW-62	650	10	24	1.353	82.668	49.905	82.479	0.069	24.0(8)	10.54(17)	-	-	
CW-78	700	6	24.5	1.417	61.169	49.985	60.795	0.271	20.6(8)	3.89(5)	19.90(13)	23.79(14)	
CW-88	700	6	51	0.473	55.180	50.021	54.713	0.382	17.0(8)	4.95(3)	11.95(3)	16.90(4)	
CW-81	700	8	24	0.794	66.168	50.087	65.896	0.167	20.9(8)	3.05(2)	21.25(7)	24.30(7)	
CW-51	700	10	48	-	70.196	50.467	69.140	0.931	24.7(8)	4.97(4)	-	-	
CW-70	700	10	26.5	1.671	68.507	50.721	67.909	0.421	34.9(8)	6.61(3)	21.16(30)	27.77(30)	
CW-82	700	12	41.3	1.318	66.910	50.681	66.052	0.486	73.3(8)	16.13(3)	67.60(22)	83.73(22)	
CW-79	700	14	41	1.080	64.876	50.187	64.183	0.540	30.5(8)	4.86(5)	32.06(9)	36.92(11)	
CW-76	700	15	26	0.763	62.728	50.127	62.066	0.332	65.8(8)	2.22(5)	60.93(13)	63.15(14)	
CW-84	700	16	24	0.569	73.811	48.945	73.274	0.339	40.4(9)	16.02(18)	26.03(12)	42.05(22)	
CW-56	750	10	48	1.756	69.586	53.048	69.258	0.126	38.8(8)	-	-	-	
CW-57	750	10	22	1.203	39.300	49.735	38.599	0.480	44.4(9)	5.19(4)	14.96(8)	20.15(9)	
CW-58	750	10	36	2.310	83.924	48.447	82.720	0.810	81.3(9)	6.95(2)	42.4(13)	49.3(13)	
CW-59	750	10	12	2.051	75.915	49.715	75.120	0.421	75.2(9)	10.44(9)	23.5(14)	33.9(14)	
CW-33	800	10	46.5	4.300	-	49.775	-	-	-	-	-	-	Melted?
CW-35	800	10	46	1.500	-	49.260	-	-	-	-	-	-	Melted
CW-60	800	10	24	1.972	79.215	49.206	77.704	1.014	100.9(9)	10.58(11)	29.28(13)	39.86(17)	Melted
CW-69	800	10	24.5	2.230	91.521	49.891	90.778	0.494	49.9(8)	11.90(19)	39.80(15)	51.70(24)	Melted

Dashes indicate values not determined. Parenthetical errors: weight-loss solubility, 1σ error propagated using $1\sigma = 0.003$ mg for each weighing step; fluid-analysis solubility, 1σ based on 3-5 ICP-AES counting periods. Type 2 crystals dissolved from inner and outer capsule surfaces

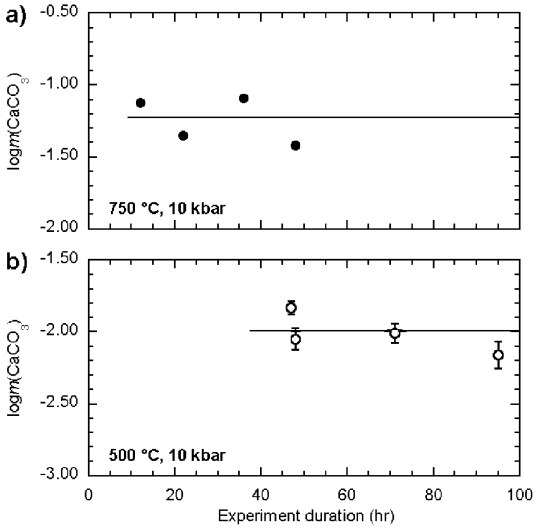

Fig. 2 **a** Logarithm of the molality of dissolved calcite vs. experiment duration at 750 °C (**a**) and 500 °C (**b**), at 10 kbar. The *horizontal line* is the mean of the replicate experiments. *Error bars*, shown where greater than symbol size, are propagated 2σ based on weighing error for each experiment

included in the weight-loss calculations, and the Ca from the dissolved type-2 crystals coating the capsules are included in calculations of fluid composition, the solubility from weight-loss measurements and the solubility calculated from fluid composition agree reasonably well. Differences for the entire experimental data set are centered on zero, indicating no systematic direction of deviation. Average absolute deviations are 27%. This supports the interpretation of run-product textures and the simplifying assumption used to calculate weight loss Eq. (5). However, compared to the rest of the data set, most results at ≥750 °C yield poor mass balance, with solubility determined by fluid analysis ~50% lower than that measured by weight-loss. This implies that it is difficult to account for all type-2 crystals where solubility is highest. Nevertheless, the general agreement between the two methods of solubility determination supports the conclusion that mass balance can be established to at least 700 °C. All following discussion of calcite solubility is based on the larger weight-loss data set.

Experiments of varying duration were conducted at 500 and 750 °C, 10 kbar, to determine the time required to achieve equilibrium. No systematic variations in calcite solubility were observed in experiments ranging from 12 to 96 h (Fig. 2). All subsequent experiments were therefore run for a minimum of 12 h.

Average analytical uncertainties from weight-loss measurements and ICP-AES analyses, when propagated through all calculations, are 8.5×10^{-4} and 3.0×10^{-4} molal, respectively, which is on the order of 1% or less. These errors are small compared to the variations observed among replicate experiments. Because of the precision differences between low- and high-temperature data, we estimated uncertainty in the 500–700 °C results separately from those at 750 and 800 °C. Uncertainty in 500–700 °C solubilities was determined by calculating the sample standard deviation, σ, from pooled replicates at individual P–T conditions (e.g., Skoog et al. 1994):

$$\sigma = \sqrt{\frac{\sum_{i=1}^{N_1}(m_i-\bar{m}_1)^2+\sum_{j=1}^{N_2}(m_j-\bar{m}_2)^2+\mathrm{K}}{N_1+N_2+\mathrm{K}}} \quad (6)$$

where m_i, N_1 and $\bar{m}_1$ are respectively the ith solubility measurement, the number of replicates and the mean solubility at P_1 and T_1, m_j, N_2 and $\bar{m}_2$ are the jth solubility measurement, the number of replicates and the mean solubility at P_2 and T_2, and so on. Six sets of two to four replicates give a pooled sample standard deviation of 0.005 molal for the weight-loss measurements. One standard deviation in the four replicate experiments at 750 °C, 10 kbar, is 0.022 molal; this was applied to experiments at ≥750 °C. The major sources of uncertainty are probably our ability to recover type-1 and type-2 crystals.

Experiments at 800 °C and 10 kbar where the initial H_2O content was greater than 95 wt% yielded type-1 crystals, quench products and an aggregate of microcrystalline, vesicular white material, interpreted as quenched melt. Wyllie and Tuttle (1960) showed that in the presence of H_2O, calcite melts incongruently at 740 °C, 1 kbar, producing a hydrous melt with a composition along the $Ca(OH)_2$–$CaCO_3$ join and a vapor phase very close to the H_2O-CO_2 join. Within the calcite + melt + vapor region the amount of melt increases with increasing H_2O content. This suggests that minute amounts of melt could have been produced with less than 95 wt% H_2O (e.g., CW-33, Table 2), but were overlooked. These results bracket the melting point of calcite in pure water at 10 kbar to between 750 and 800 °C.

Figure 3 shows calcite solubility as a function of temperature and pressure. At the high P of this study, the solubility of calcite increases with increasing T. At 10 kbar, calcite solubility increases from 1.6×10^{-2} molal at 500 °C to 5.7×10^{-2} molal at 750 °C. Our data confirm the progressive change from isobaric decrease to isobaric increase in calcite solubility with increasing P implied by low-P experimental data (Walther and Long 1986; Fein and Walther 1989).

Isothermal plots at 500, 600 and 700 °C (Fig. 4) reveal that calcite solubility is only weakly dependent on P at >6 kbar. Combined with the results of Walther and Long (1986) and Fein and Walther (1989), a strong P dependence is indicated at <6 kbar; for example, between 1 and 6 kbar, 500 °C, calcite solubility increases more than two orders of magnitude, from $1.8\text{x }10^{-5}$ to 6.4×10^{-3} molal. By contrast, at >6 kbar, calcite solubility increases less than one order of magnitude, from 6.4×10^{-3} to 1.7×10^{-2} molal at the same T. Note that the large pressure dependence required by the 500 and 600 °C data leads to prediction of similar behavior at

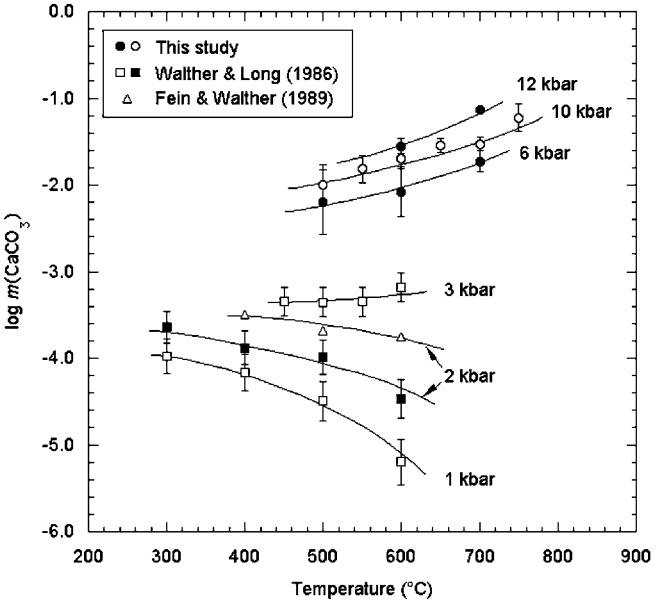

Fig. 3 Log m_{CaCO3} vs. temperature for experiments at selected pressures showing results of this study and previous work. At those *P–T* where experiments were repeated, averages of all experiments are plotted. *Error bars* for results of this study are 1σ based on pooled results (< 750 °C) or 1σ in the mean (750 °C; see text); those for Walther and Long (1986) are 5% relative uncertainty. The *curves* were visually fit to the data

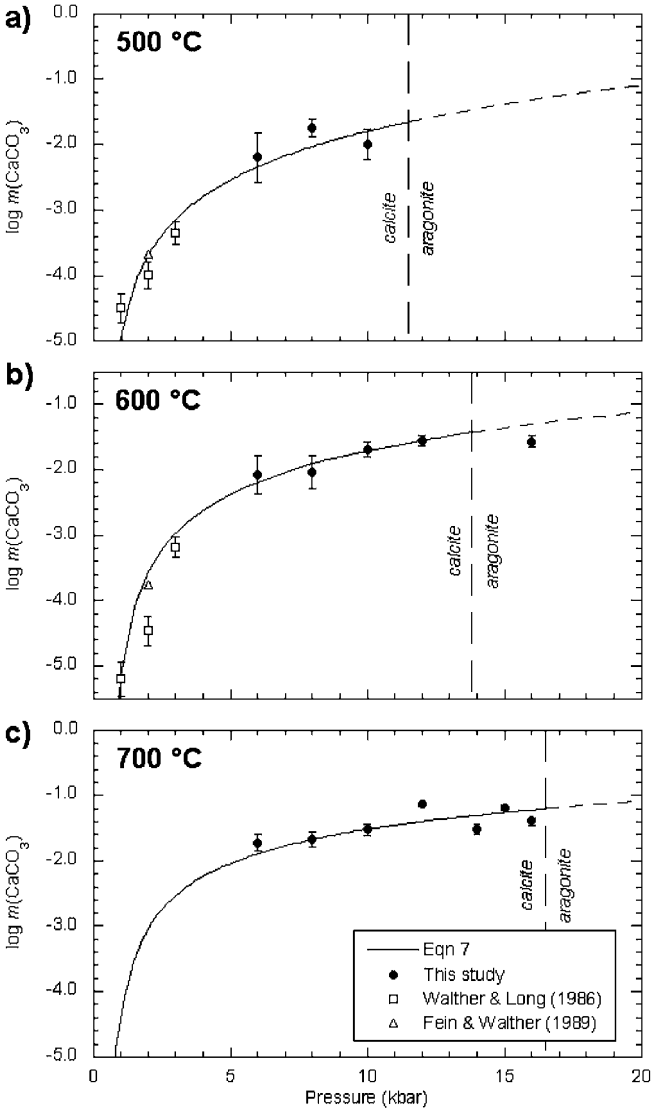

Fig. 4 Log m_{CaCO3} vs. pressure for experiments at 500 (**a**), 600(**b**) and 700 °C (**c**). *Curves* calculated from Eq. (7). Calcite-aragonite transition is from Holland and Powell (1998). *Dashed lines* indicate extrapolated, metastable calcite solubility within the aragonite stability field. *Error bars* as in Fig. 3

700 °C (Fig. 4c), although no measurements have been made below 6 kbar at this temperature.

One solubility measurement was conducted within the aragonite stability field at 600 °C, 16 kbar (CW-90, Table 2). This experiment resulted in a dense aggregate of sugary-textured crystals, interpreted to be aragonite, although no x-ray studies were conducted to confirm this. Conversion of calcite to aragonite should have occurred in minutes at the conditions of this experiment (Johannes and Puhan 1971; Boettcher and Wyllie 1968). Therefore, it is likely that the experiment measured the solubility of aragonite, not metastable calcite. The solubility determined within the aragonite stability field is within error of that for stable calcite at 12 kbar, 600 °C.

Discussion

Calcite solubility as a function of *T* and *P*

The results of the present study can be combined with previous work to constrain calcite solubility in H_2O over a wide range of *P* and *T* (Fig. 4). Fein and Walther (1989) suggested that the results of Walther and Long (1986) were 0.3–0.5 log molality units too low at any given *P–T*. They explain this change by improvement in sample collection method used. However, Fig. 4 illustrates that this discrepancy is small compared to the large changes with *P* from 1 to > 10 kbar. The combined low-*P* and high-*P* data sets show that measured calcite solubility at constant *T* is a linear function of the logarithm of the density of water, consistent with previous experimental work on other systems (Eugster and Baumgartner 1987; Mesmer et al. 1988; Anderson et al. 1991, Manning 1994). Therefore the results of this study and those of Fein and Walther (1989) were regressed to give:

$$\log m_{CaCO_3} = -3.95 + 0.00266T + (32.8 - 0.0280T)\log \rho_{H_2O} \quad (7)$$

where *T* is in Kelvin and ρ_{H2O} is the density of water in g/cm^3. Solubility calculated from Eq. (7) is also shown in Fig. 4. Equation (7) reproduces experimental results between 400 and 750 °C and 1 to 16 kbar with a mean relative deviation of 10%. Despite accuracy concerns, the data of Walther and Long (1986) are also broadly

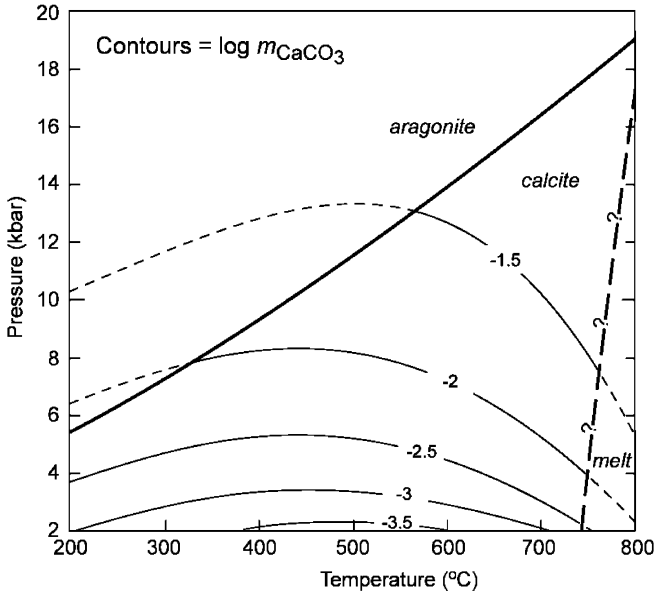

Fig. 5 Contours of log m_{CaCO3} (Eq. 7) as a function of pressure and temperature. Calcite-aragonite transition is from Holland and Powell (1998). The provisional water-saturated solidus is based on Wyllie and Tuttle (1960) and this study (Table 2). *Short-dashed isopleths* indicate metastable calcite solubility within aragonite or melt stability fields

consistent with the fit, although they were not used to derive the equation. Regression based on water density means that the fit probably extrapolates well to the upper stability of calcite in the presence of water at the aragonite-calcite-melt-H_2O invariant point at about 20 kbar and 800 °C.

Isopleths of calcite solubility calculated from Eq. (7) , Fig. (5) illustrate the nature of the T and P dependence of calcite dissolution behavior. Individual isopleths display maxima, which increase from ~450 to ~500 °C as P increases. The trace of the calcite-aragonite equilibrium intersects the maximum in solubility isopleths at ~log $m_{CaCO3} = -1.7$ (~11 kbar). Below this P, an isobaric increase in T causes a decrease in calcite solubility up to ~500 °C. Thus the well-known isobaric "reverse solubility" of calcite (decreasing solubility with increasing T) persists to ~11 kbar. If the metastable isopleths of calcite solubility in the aragonite stability field are a reasonable approximation of aragonite solubility behavior, we predict that a maximum in the isopleths, hence reverse-solubility behavior, will persist for aragonite at least to 20 kbar. Our results suggest that above 2 kbar, isobaric T increases at $T > 500$ °C yield an increase in calcite solubility. The generally shallow positive or negative slopes of solubility isopleths at < 600 °C indicate that in this T range, P has a stronger effect on calcite solubility than T. However, the steep negative slopes of isopleths above ~600 °C indicate that at high T, calcite solubility is strongly dependent on both P and T.

The calcite-solubility isopleths (Fig. 5) are in marked contrast to those for quartz at high pressures, which are rather steep P–T isopleths due to the very strong temperature dependence on solubility (Manning 1994). This suggests that quartz and calcite dissolution or precipitation may occur along different sections of a given burial-uplift path, which in turn will vary with the tectonic environment.

Speciation

Experiments on calcite solubility in H_2O do not uniquely constrain species concentrations; however, a provisional estimate can be derived by comparison with data at low P. Fein and Walther (1987) used experimentally determined calcite solubility in H_2O-CO_2 fluids to assess species abundance and to adjust the standard molal Gibbs free energy of $CO_{2,aq}$ at high P and T ($\Delta G^{\circ}_{CO_{2,aq}}$). Their results indicate that at the conditions of their experiments, $\Delta G^{\circ}_{CO_{2,aq}}$ required revision, whereas $\Delta G^{\circ}_{HCO_3^-}$ values are accurate. This can be seen by comparing equilibrium constants (K) for equilibrium (1) with those for:

$$\underset{\text{calcite}}{CaCO_3} + H^+ = Ca^{+2} + HCO_3^- \qquad (8)$$

as constrained by experiments (Fein and Walther 1987, 1989) and calculated (SUPCRT92; Johnson et al. 1992) from tabulated thermodynamic data (Helgeson et al. 1978; Shock et al. 1997). Table 3 shows that, at 1 and 2 kbar, 500 °C, there is good agreement between predicted and experimentally constrained log K_8, but that log K_1 as constrained by experiment is significantly lower than predicted. Fein and Walther's (1987) approach can be extended to high P by using our calcite solubility measurements to compute the abundance and thermodynamic properties of $CO_{2,aq}$. However, because the modified Helgeson-Kirkham-Flowers equation of state for aqueous species used in SUPCRT92 can be used only at ≤ 5 kbar, extrapolation is necessary. It has been shown that the logarithm of the equilibrium constant for many mineral hydrolysis reactions is linear with log ρ_{H_2O} at constant T (Eugster and Baumgartner 1987; Mesmer et al. 1988; Anderson et al. 1991; Manning 1994, 1995). Figure 6 shows log K_8 vs. log ρ_{H_2O} at 500–700 °C, 2–5 kbar, calculated at 0.5 kbar increments using SUPCRT92 with data for aqueous species from Shock et al. (1997). Error bars correspond to estimated

Table 3 Values of logK_1 and logK_8 from previous work at 500 °C

P (kbar)	Log K_1			Log K_8		
	SUPCRT92	FW87	FW89	SUPCRT92	FW87	FW89
1	6.87	4.79		−4.05	−4.24	
2	6.85	4.92	5.6	−3.01	−2.55	−2.2

SUPCRT92 values calculated using updated data from Shock et al. (1997); FW87, Fein and Walther (1987); FW89, Fein and Walther (1989). Standard state for aqueous species is unit activity of the hypothetical 1 molal solution at infinite dilution; for minerals and H_2O, it is the pure phase at any P and T

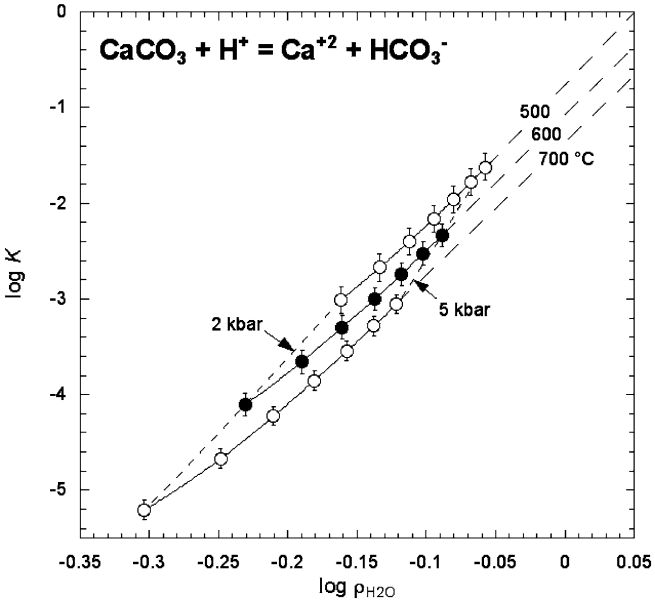

Fig. 6 Extrapolation of the equilibrium constant for Eq. (8) as a function of the logarithm of water density. Individual data points are values at 0.5 kbar increments from 2–5 kbar, 500, 600 and 700 °C, calculated from SUPCRT92 using data of Shock et al. (1997). Uncertainties correspond to 500 cal/mol. *Long dashed lines* show linear extrapolation to > 5 kbar (see text). *Short dashed lines* are selected isobars (2 and 5 kbar)

uncertainties of 0.5 kcal/mol in ΔG°_{PT} of reaction (Shock et al. 1997). As H_2O density and P increase, the change in log K_8 vs. log ρ_{H_2O} becomes linear (Fig. 6), implying that:

$$\left(\frac{\partial \ln K_8}{\partial \ln \rho_{H_2O}}\right) = -\frac{\Delta_r V^{\circ}_8}{\beta_{H_2O} RT} = \text{constant} \tag{9}$$

where ρ_{H_2O} and β_{H_2O} are the density and isothermal compressibility of water, R is the gas constant, T is temperature in Kelvin and $\Delta_r V^{\circ}_8$ is the standard molar volume of Eq. (8). Figure 6 shows that, within the uncertainties in log K, a linear extrapolation to high P is appropriate. We calculated values for $-\Delta_r V^{\circ}_8/\beta_{H_2O}RT$ at 5 kbar of 15.1, 14.2 and 13.9 at 500, 600, and 700 °C and used these values to determine log K_8 at $P > 5$ kbar. To assess species predominance in our experiments, we initially considered five species Ca^{+2}, $CO_{2,aq}$, HCO_3^-, H^+ and OH^-. If we adopt a standard state for minerals and H_2O of unit activity of the pure phase at any P and T, then for a given P and T the experimentally determined calcite solubility and the equilibrium constants for reactions (3), (4) and (8), yield the following equations:

$$K_4 = a_{H^+} a_{OH^-} \tag{10}$$

$$K_8 = \frac{a_{Ca^{+2}} a_{HCO_3^-}}{a_{H^+}} \tag{11}$$

$$m_{Ca} = m_{CO_{2,aq}} + m_{HCO_3^-} \tag{12}$$

$$2m_{Ca^{+2}} + m_{H^+} = m_{HCO_3^-} + m_{OH^-} \tag{13}$$

Equations (10), (11), (12), and (13) and expressions for activity coefficients of charged species (Davies 1962) were solved by iteration, assuming unit activity coefficients for neutral species and adopting a value for the Debye-Hückel paramater (A) of 1.0 $kg^{1/2}mol^{-1/2}$ at > 5 kbar, which is justified because speciation calculations are not sensitive to A at high P. At ≤ 5 kbar, A was taken from Helgeson and Kirkham (1974). The equilibrium constant for H_2O dissociation was calculated from Marshall and Frank (1981). The standard state for aqueous species is unit activity of the hypothetical one molal solution referenced to infinite dilution. Simultaneous solution of the system of equations at each experimental condition reveals that $CO_{2,aq}$ is the dominant carbonate species (> 98.6%) at all experimental conditions. Fein and Walther (1987, 1989) obtained a similar result at 1 and 2 kbar. Calculated pH ranges from 5.5 to 6.9.

Fein and Walther (1987, 1989) concluded that $CaOH^+$ was not a significant Ca species in calcite-saturated H_2O at 1–2 kbar. Since their work, new predicted thermodynamic data for $CaOH^+$ were reported (Shock et al. 1997). Using the Shock et al. (1997) data, the equilibrium constant for

$$Ca^{+2} + H_2O = CaOH^+ + H^+ \tag{14}$$

was estimated by the same methods as for Eq. (8), which permits speciation of the experimental fluids with inclusion of $CaOH^+$. Results indicate that $CaOH^+$ should be similar to or predominate over Ca^{+2} (58–99%). The predominance of $CaOH^+$ over Ca^{+2} results from a larger value for K_{14} derived from Shock et al. (1997) than was inferred by Fein and Walther (1987). The Shock et al. (1997) data also predict that $CaOH^+$ predominates in calcite-saturated H_2O at 1–2 kbar; however, Fein and Walther (1987) suggested that this is inconsistent with experimentally constrained values of K_2 at low T (Read 1975). However, regardless of this discrepancy, $CO_{2,aq}$ remains the most abundant C-bearing species (> 97%) when $CaOH^+$ is included, and there is only a small shift in pH ranges from 5.4–6.6. Thus, although our data cannot constrain the relative abundance of Ca species, we can conclude that uncertainty in their distribution does not affect the inference that $CO_{2,aq}$ predominates.

The additional species CO_3^{-2}, $CaHCO_3^+$ and $CaCO_{3,aq}$ (Shock et al. 1997; Sverjensky et al. 1997) were also considered by extrapolation of the equilibrium constants for Eq. (3) as well as:

$$CaHCO_3^+ = Ca^{+2} + HCO_3^- \tag{15}$$

and

$$CaCO_{3,aq} + H^+ = Ca^{+2} + HCO_3^- \tag{16}$$

to > 5 kbar. Using extrapolated log K values to expand the speciation calculations to nine species indicates that

CO_3^{-2}, $CaHCO_3^+$ and $CaCO_{3,aq}$ are not significant ($< < 1\%$) in any of the experimental fluids.

The speciation calculations show that, regardless of discrepancies in predicted abundance of $CaOH^+$, and provided that other thermodynamic data and the extrapolation scheme are accurate, we can conclude that the dominant form of dissolved carbon in calcite-saturated H_2O at 500–750 °C and P up to at least 16 kbar is the neutral $CO_{2,aq}$ species. Because the system of equations does not depend on the problematic thermodynamic properties of $CO_{2,aq}$, the calculations should be robust, provided that the extrapolations are not in error by more than the uncertainty in the standard state thermodynamic properties of the other aqueous species.

Thermodynamic properties of Eq. (1)

Results of the speciation calculations above yield the equilibrium constant for Eq. (1) via:

$$K_1 = \frac{a_{Ca^{+2}} a_{CO_{2,aq}}}{a^2_{H^+}} \quad (17)$$

Figure 7 shows log K_1 at 500 °C as a function of pressure. Fein and Walther (1987, 1989) reported K_1 assuming all Ca as Ca^{+2}. Using this assumption and solubilities calculated using Eq. (7), our results require that log K_1 increase strongly with P, from ~4 at 1 kbar to ~8 at 6–10 kbar, consistent with the large pressure dependence of calcite solubility. Values of log K_1 from Fein and Walther (1987, 1989) and this study recalculated including $CaOH^+$ are lower (Fig. 7), but the strong P dependence remains. By contrast, log K_1 computed from SUPCRT92 ($CO_{2,aq}$ from Shock et al. 1989) and extrapolated to high P using the methods described above implies that calcite solubility should display little pressure dependence (Fig. 7). This behavior is clearly inconsistent with the experimental data.

Although temperature does not have as strong an effect on calcite solubility as pressure, the observation of isobaric increases in calcite solubility with increasing T implies larger standard molal enthalpy ($\Delta_r H°$) and entropy ($\Delta_r S°$) of Eq. (1) at high T and P than previously recognized. For example, using calcite solubility calculated from Eq. (7) at 5 kbar, fluid speciation calculations allow determination of log K_1 as a function of T. Speciation without $CaOH^+$ yields $\Delta_r H^\circ_1$ and $\Delta_r S^\circ_1$ of 190 and 180 J/mol K respectively at 500–800 °C. Consideration of $CaOH^+$ lowers these values to 140 kJ/mol and 150 J/mol K. Either way, $\Delta_r H^\circ_1$ and $\Delta_r S^\circ_1$ constrained by high-P experiments are substantially larger than the values of 37 and 43 J/mol K calculated from predicted thermodynamic data (Shock et al. 1989). The difference results from isobaric temperature dependence of calcite solubility determined experimentally.

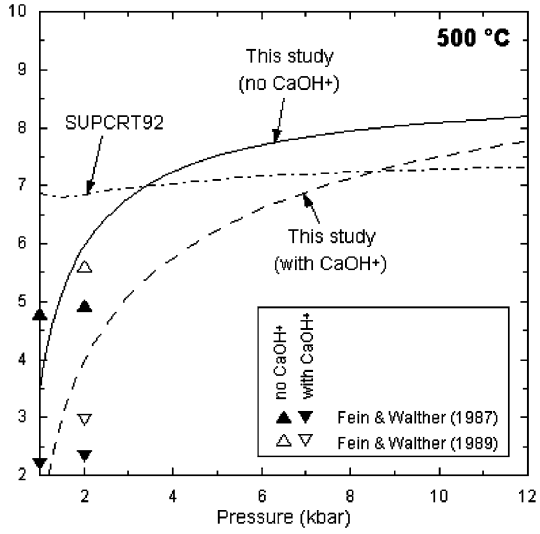

Fig. 7 Log K_1 vs. pressure at 500 °C. Log K_1 calculated using calcite solubility from Eq. (7) and speciation with and without $CaOH^+$ is shown with *dashed* and *solid curves*, respectively. *Upward pointing triangles* show log K_1 values from Fein and Walther (1987, 1989). *Downward pointing triangles* are the same values recalculated by including $CaOH^+$. The *dash-dot curve* shows log K_1 calculated with SUPCRT92 (Johnson et al. 1992) using data from Shock et al. (1989, 1997), with extrapolation to > 5 kbar (see text). Experimental results require that log K_1 depends more strongly on P than predicted

Conclusions

New measurements of the solubility of calcite in pure water show that calcite dissolves congruently between 6–16 kbar and 500 and 750 °C. The dominant carbonate species at these conditions is determined to be $CO_{2,aq}$. Calcite solubility is strongly dependent on P, but only weakly T dependent. This behavior, which was not predicted from existing thermodynamic data, has important geologic consequences. Fluid flow involving large changes in P can be important in influencing CO_2 metasomatism and transport. H_2O evolved at depth and rising in the crust will become progressively less able to hold calcite in solution. Thus, a substantial fraction of lower-crust-derived CO_2 can be retained by the crust via calcite precipitation along the flow path, rather than degassed at the surface.

Acknowledgements This research was supported by NSF-EAR 9909583. Reviews by D. Kerrick and J. Walther substantially improved the manuscript. Many thanks to Bob Newton and Heather Lin for their help in the UCLA high-pressure lab and also to Amir Liba for his assistance with the ICP-AES analyses at UCLA.

References

Anderson GM, Burnham CW (1965) The solubility of quartz in super-critical water. Am J Sci 263:494–511

Anderson GM, Castet S, Schott J, Mesmer RE (1991) The density model for estimation of thermodynamic parameters of reactions

at high temperatures and pressures. Geochim Cosmochim Acta 55:1769–1779
Boettcher AL, Wyllie PJ (1968) The calcite-aragonite transition measured in the system $CaO–CO_2–H_2O$. J Geol 76:314–330
Bohlen SR (1984) Equilibria for precise pressure calibration and a frictionless furnace assembly for the piston-cylinder apparatus. Neues Jahrb Miner Monatsh 9:404–412
Bond WL (1951) Making small spheres. Rev Sci Instrum 22:344–345
Boyd FR, England JL (1960) Apparatus for phase-equilibrium measurements at pressures up to 50 kilobars and temperatures up to 1,750 degrees C. J Geophys Res 65:741–748
Davies CW (1962) Ion association. Butterworths, Washington, DC, 190 pp
Ellis AJ (1959) The solubility of calcite in carbon dioxide solutions. Am J Sci 257:354–365
Ellis AJ (1963) The solubility of calcite in sodium chloride solutions at high temperatures. Am J Sci 261:259–267
Eugster HP, Bumgartner L (1987) Mineral solubilities and speciation in supercritical metamorphic fluids. In: Carmichael ISE, Eugster HP (eds) Thermodynamic modeling of geologic materials: minerals, fluids and melts. Rev Mineral 17:367–403
Fein JB, Walther JV (1987) Calcite solubility in supercritical CO_2-H_2O fluids. Geochim Cosmochim Acta 51:1665–1673
Fein JB, Walther JV (1989) Calcite solubility and speciation in supercritical NaCl-HCl aqueous fluids. Contrib Mineral Petrol 103:317–324
Frear GL, Johnston J (1929) The solubility of calcium carbonate (calcite) in certain aqueous solutions at 25 °C. J Am Chem Soc 51:2082–2092
Helgeson HC, Kirkham DH (1974) Theoretical prediction of the thermodynamic behavior of aqueous electrolytes at high pressures and temperatures. II. Debye-Huckel parameters for activity coefficients and relative partial molal properties. Am J Sci 274:1199–1261
Helgeson HC, Delaney JM, Nesbitt HW, Bird DK (1978) Summary and critique of the thermodynamic properties of rock-forming minerals. Am J Sci 278-A: 1–229
Holland TJB, Powell R (1991) A compensated-Redlich-Kwong (CORK) equation for volumes and fugacities of CO_2 and H_2O in the range 1 bar to 50 kbar and 100–1,600 °C. Contrib Mineral Petrol 109:265–273
Holland TJB, Powell R (1998) An internally consistent thermodynamic data set for phases of petrological interest. J Metamorph Geol 16:309–343
Johannes W (1973) A simplified piston-cylinder apparatus of high precision. Neues Jahrb Miner Monatsh 7/8:331–351
Johannes W, Puhan D (1971) The calcite-aragonite transition, reinvestigated. Contrib Mineral Petrol 31:28–38
Johnson JW (1992) SUPCRT92: A software package for calculating standard molal thermodynamic properties of minerals, gases, aqueous species, and reactions from 1 to 5,000 bar and 0 to 1,000 °C. Comp Geosci 18:899–947
Kerrick DM, Connolly JAD (2001) Metamorphic devolatilization of subducted oceanic metabasalts; implications for seismicity, arc magmatism and volatile recycling. Earth Planet Sci Lett 189:19–29
Malinin SD, Kanukov AB (1972) The solubility of calcite in homogeneous $H_2O–NaCl–CO_2$ systems in the 200–600 degrees C temperature interval. Geochem Int 8:668–679
Manning CE (1994) The solubility of quartz in H_2O in the lower crust and upper mantle. Geochim Cosmochim Acta 58:4831–4839
Manning CE (1995) Phase-equilibrium controls on SiO_2 metasomatism by aqueous fluids in subduction zones: reaction at constant pressure and temperature. Int Geol Rev 37:1074–1093
Manning, CE, Boettcher SL (1994) Rapid-quench hydrothermal experiments at mantle pressures and temperatures. Am Mineral 79:1153–1158
Marshall WL, Franck EU (1981) Ion product of water substance, 0–1,000 °C, 1–10,000 bars, new international formulation and its background. J Phys Chem Ref Data 10:295–304
Mesmer RE, Marshall WL, Palmer DA, Simonson JM, Holmes HF (1988) Thermodynamics of aqueous association and ionization reactions at high temperatures and pressures. J Sol Chem 1:699–718
Miller JP (1952) A portion of the system calcium carbonate-carbon dioxide-water, with geological implications. Am J Sci 250:161–203
Morey GW (1962) The action of water on calcite, magnesite and dolomite. Am Mineral 47:1456–1460
Newton RC, Manning CE (2000) Quartz solubility in $H_2O–NaCl$ and $H_2O–CO_2$ solutions at deep crust-upper mantle pressures and temperatures: 2–15 kbar and 500–900 °C. Geochim Cosmochim Acta 64:2993–3005
Newton RC, Manning CE (2002) Experimental determination of calcite solubility in H_2O-NaCl solutions at deep crust/upper mantle pressures and temperatures: implications for metasomatic processes in shear zones. Am Mineral 87:1401–1409
Plummer LN, Busenberg E (1982) The solubilities of calcite, aragonite and vaterite in $CO_2–H_2O$ solutions between 0 and 90 °C, and an evaluation of the aqueous model for the system $CaCO_3–CO_2–H_2O$. Geochim Cosmochim Acta 46:1011–1040
Read AJ (1975) The first ionization constant of carbonic acid from 25 to 250 °C and to 2,000 bar. J Sol Chem 4:53–70
Schloemer VH (1952) Hydrothermale Untersuchungen über das System $CaO–MgO–CO_2–H_2O$. Neues Jahrb Miner Monatsh 129–135
Segnit ER, Holland HD, Biscardi CJ (1962) The solubility of calcite in aqueous solutions; I, The solubility of calcite in water between 75 degrees and 200 degrees at CO_2 pressures up to 60 atm. Geochim Cosmochim Acta 26:1301–1331
Sharp WE, Kennedy GC (1965) The system CaO-CO_2-H_2O in the two-phase region calcite + aqueous solution. J Geol 73:391–403
Skoog DA West DM, Holler FT (1994) Analytical chemistry. Harcourt Brace, Orlando
Shock EL, Sassani DC, Willis M, Sverjensky DA (1997) Inorganic species in geologic fluids: correlations among standard molal thermodynamic properties of aqueous ion and hydroxide complexes. Geochim Cosmochim Acta 61:907–950
Shock EL, Helegeson HC, Sverjensky DA (1989) Calculation of the thermodynamic and transport properties of aqueous species at high pressures and temperatures: standard partial molal properties of inorganic neutral species. Geochim Cosmochim Acta 53:2157–2183
Sverjensky DA, Shock EL, Helegeson, HC (1997) Prediction of the thermodynamic properties of aqueous metal complexes to 1,000 °C and 5 kb. Geochim Cosmochim Acta 61:1359–1412
Walther JV, Long MI (1986) Experimental determination of calcite solubilities in supercritical H_2O. Fifth International Symposium on Water–rock interaction 5:609–611
Wells RC (1915) The solubility of calcite in water in contact with the atmosphere and its variation with temperature. J Wash Acad Sci 5:617–622
Wyllie PJ, Tuttle OF (1960) The system CaO-CO_2-H_2O and the origin of carbonatites. J Petrol 1:1–46